Supplemental Document

OPTICA QUANTUM

Enhancing upconversion with space–time entanglement: from twin photons to twin-beams: supplement

ALESSANDRA GATTI,[1,*] MATTEO CLERICI,[2] AND LUCIA CASPANI[2]

[1] *Istituto di Fotonica e Nanotecnologie del CNR, Piazza Leonardo da Vinci 32, Milano, Italy*
[2] *Como Lake Institute of Photonics, Dipartimento di Scienza e Alta Tecnologia,Universita' degli Studi dell'Insubria, Via Valleggio 11, Como, Italy*
[*] *Alessandra.Gatti@ifn.cnr.it*

Supplement DOI: https://doi.org/10.6084/m9.figshare.29075006

Parent Article DOI: https://doi.org/10.1364/OPTICAQ.554539

Enhancing upconversion with space-time entanglement: from twin photons to twin-beams. Supplemental document

This document contains supplementary information in support of the manuscript "Enhancing upconversion with space-time entanglement: from twin photons to twin beams". It provides the mathematical derivation of the equations (22-25) of the main manuscript, and supplies a detailed comparison between the quantum and classical efficiencies of second harmonic generation in the pulsed case.

INTRODUCTION

Section 1 provides a derivation of the equations (22-25) of the main manuscript for the intensity of the second harmonic (SH) signal generated by upconverting photons from parametric down-conversion (PDC). This derivation generalizes the quasi-stationary approximation used for describing PDC in [1, 2] to the second harmonic generation (SHG) process.
Section 2 focuses on the comparison of the quantum and classical SHG efficiencies, providing more details on the pulsed case, in which the total energy of the SH pulse is measured.

1. ENTANGLED SHG IN THE QUASI-STATIONARY APPROXIMATION: DERIVATION OF EQUATIONS (22-25)

Our starting point is the equation (22) for the the coherence function of the second harmonic field $\hat{A}_2$ generated at the output of the NL_2 medium, which we rewrite as:

$$\left\langle \hat{A}_2^\dagger(w_0')\hat{A}_2(\vec{w}_0)\right\rangle = e^{i[k_{2z}(\vec{w}_0)-k_{2z}(\vec{w}_0')]l_c'}\left\langle \hat{a}_2^\dagger(w_0')\hat{a}_2(\vec{w}_0)\right\rangle \tag{S1}$$

$$\left\langle \hat{a}_2^\dagger(w_0')\hat{a}_2(\vec{w}_0)\right\rangle = \int\int \frac{d^3w\, d^3w'}{(2\pi)^3}\Big[\,\Phi_{\mathrm{SHG}}^*(\vec{w}',\vec{w}_0'-\vec{w}')\Phi_{\mathrm{SHG}}(\vec{w},\vec{w}_0-\vec{w}) \times\left\langle \hat{B}_1^\dagger(\vec{w}')\hat{B}_1^\dagger(\vec{w}_0'-\vec{w}')\hat{B}_1(\vec{w})\hat{B}_1(\vec{w}_0-\vec{w})\right\rangle\Big] \tag{S2}$$

where we remind that $\vec{w}$ is the Fourier coordinate (q_x, q_y, Ω) in $\mathbb{R}^3$. The SH intensity distribution in the space-time domain $\vec{\xi} = (x, y, t)$ will be obtained by Fourier transforming:

$$\left\langle \hat{A}_2^\dagger(\vec{\xi})\hat{A}_2(\vec{\xi})\right\rangle = \int\int \frac{d^3w_0\, d^3w_0'}{(2\pi)^3}\left\langle \hat{A}_2^\dagger(w_0')\hat{A}_2(\vec{w}_0)\right\rangle e^{i\vec{\xi}\cdot(\vec{w}_0-\vec{w}_0')} \tag{S3}$$

In the case of quantum illumination, the input fundamental field $\hat{B}_1$ is the output of the PDC process in NL_1 , which has propagated through the imaging system, according to the linear transformation (21). Then, the Gaussian factorization theorem can be used in order to recast its normally ordered fourth order moment in terms of the second order moments:

$$\begin{aligned}\langle \hat{B}_1^\dagger(\vec{w}')\hat{B}_1^\dagger(\vec{w}_0'-\vec{w}')\hat{B}_1(\vec{w})\hat{B}_1(\vec{w}_0-\vec{w})\rangle =& \langle \hat{B}_1^\dagger(\vec{w}')\hat{B}_1^\dagger(\vec{w}_0'-\vec{w}')\rangle\langle \hat{B}_1(\vec{w})\hat{B}_1(\vec{w}_0-\vec{w})\rangle \\ &+ \langle \hat{B}_1^\dagger(\vec{w}')\hat{B}_1(\vec{w})\rangle\langle \hat{B}_1^\dagger(\vec{w}_0'-\vec{w}')\hat{B}_1(\vec{w}_0-\vec{w})\rangle \\ &+ \langle \hat{B}_1^\dagger(\vec{w}')\hat{B}_1(\vec{w}_0-\vec{w})\rangle\langle \hat{B}_1^\dagger(\vec{w}_0'-\vec{w}')\hat{B}_1(\vec{w})\rangle\end{aligned} \tag{S4}$$

where the first term originates from entangled photon pairs, and gives rise to the coherent component of the SH field, while the other two terms originate from nonentangled pairs and would be present also in the case of a multithermal input state.

A. Coherent component

Let' s start from the first term at the r.h.s. of Eq. (S4). By insertingt into Eq. (S2), the result factorizes into:

$$\left\langle \hat{a}_2^\dagger(w_0')\hat{a}_2(\vec{w}_0)\right\rangle^{Ent} = \langle \hat{a}_2^\dagger(w_0')\rangle \langle \hat{a}_2(\vec{w}_0)\rangle \tag{S5}$$

where

$$\langle \hat{a}_2(\vec{w}_0)\rangle = \int \frac{d^3w}{(2\pi)^{\frac{3}{2}}}\Phi_{\mathrm{SHG}}(\vec{w},\vec{w}_0-\vec{w})\langle \hat{B}_1(\vec{w})\hat{B}_1(\vec{w}_0-\vec{w})\rangle \tag{S6}$$

is (up to a phase factor) the expectation value of the second harmonic field, and constitutes its coherent component. The biphoton amplitude at the NL_2 input is then rewritten in terms of the biphoton amplitude at the PDC crystal output by using the propagator in Eq. (21):

$$\langle \hat{B}_1(\vec{w})\hat{B}_1(\vec{w}_0-\vec{w})\rangle = \chi_F(\Omega)\chi_F(\Omega_0-\Omega)h^{\Delta z}(\vec{w})h^{\Delta z}(\vec{w}_0-\vec{w})\langle \hat{C}_1(\vec{w})\hat{C}_1(\vec{w}_0-\vec{w})\rangle, \tag{S7}$$

where

$$h^{\Delta z}(\vec{w}) = \exp\left(i\frac{\Delta z}{2k_{1v}}\frac{q^2}{1+\frac{\Omega}{\omega_1}}\right) \tag{S8}$$

describes the paraxial propagation from NL_1 to NL_2 throught the 4 imaging system, and corresponds to the backward propagation from the image plane at $z=\Delta z$ to the input plane $z=0$ of NL_2;

$$\chi_F(\Omega) = \mathrm{rect}(\frac{\Omega}{\Delta\Omega}) = \begin{cases} 1 & \text{for } \Omega \in \left(-\frac{\Delta\Omega}{2},\frac{\Delta\Omega}{2}\right) \\ 0 & \text{elsewhere} \end{cases}$$

simulates a rectangular bandpass filter of width $\Delta\Omega$ around ω_1.

Let us now assume the validity of the quasi-stationary (QS) approximation under which the QS model for PDC was derived [1, 2]. By Fourier transforming the space-time biphoton correlation in Eq.(9), one has

$$\left\langle \hat{C}_1(\vec{w})\hat{C}_1(\vec{w}_0-\vec{w})\right\rangle = \mu_{corr}(\vec{w}_0)\Phi_{\mathrm{PDC}}(\vec{w},-\vec{w}), \tag{S9}$$

where $\Phi_{\mathrm{PDC}}(\vec{w},-\vec{w})$ is the Fourier distribution of biphotons, defined in Eq. (14), which varies on the *slow* scales $\Omega_{\mathrm{D}} = \frac{1}{\sqrt{k_1'' l_c}}$ and $Q_{\mathrm{D}} = \sqrt{\frac{k_1}{l_c}}$, associated with temporal dispersion and diffraction along NL_1 (see Fig. 2a). On the other side,

$$\mu_{corr}(\vec{w}) = \int \frac{d^3\xi}{(2\pi)^3}F_{corr}(\xi)e^{-i\vec{w}\cdot\vec{\xi}}, \qquad \text{with } F_{corr}(\vec{\xi}) = \frac{\sinh\left(2g\mathcal{A}_p(\vec{\xi})\right)}{\sinh\left(2g\right)}, \tag{S10}$$

is a well localized correlation peak, which, as discussed in detail in [1], has a *fast* decay on the scales

$$\Omega_{corr} = \frac{1}{\tau_p}\sqrt{\frac{4g}{\tanh(2g)}} \ll \Omega_{\mathrm{D}}, \qquad q_{corr} = \frac{1}{w_p}\sqrt{\frac{4g}{\tanh\left(2g\right)}} \ll Q_{\mathrm{D}}, \tag{S11}$$

where without losing of generality we assumed a Gaussian pump field of the form $\mathcal{A}_p(\vec{r},t) = \exp(-\frac{r^2}{D_p^2}-\frac{t^2}{\tau_p^2})$. In the following, we shall refer to the narrow region occupied by the correlation peak (S10) as the *fast* domain $\mathcal{S}_0$. Equation (S11) is the fundamental ansatz of the QS model [2]: it requires not only that the pump duration and cross-section are much larger than the temporal and spatial broadening due to dispersion and diffraction in the medium: $\tau_p \gg \tau_{\mathrm{D}} = \sqrt{k_1'' l_c}$, and $w_p \gg l_{\mathrm{D}} = \sqrt{\frac{l_c}{k_1}}$, but also that the generated PDC pulse still satisfies the same requirements after the exponential shrinking: $\tau_p\sqrt{\frac{\tanh(2g)}{2g}} \gg \tau_{\mathrm{D}}$ and $w_p\sqrt{\frac{\tanh(2g)}{2g}} \gg l_{\mathrm{D}}$. These conditions are typically not difficult to meet: for example, for the 2 mm BBO considered in the main manuscript (see Fig. (2)), $\tau_{\mathrm{D}} = 9.4\,\mathrm{fs}$ and $l_{\mathrm{D}} = 14\,\mu\mathrm{m}$, so standard laser pulses, with durations $> 100\,\mathrm{fs}$, satisfy them. A further assumption, that allows to derive a simpler and quasi analytical QS model, is that the effects of the GVM and of the transverse walk-off between the pump and signal waves are not too large. This requires that the pump pulse is not shorter than the GVM time delay $\tau_{\mathrm{GVM}} = (k_2' - k_1')l_{\mathrm{c}}$ and its cross-section is not narrower than the the walk-off distance $l_{\mathrm{wo}} = \rho l_{\mathrm{c}}$,

where ρ is the walk-off angle of the Poynting vector. For the 2 mm BBO considered in the main manuscript, $\tau_{\rm GVM} = 185 fs$, and $l_{\rm wo} = 113\,\mu$m, hence these conditions might be not precisely satisfied, and some care should be taken to evaluate the effects of GVM for shorter lase pulses. Nevertheless, the effects of GVM, if not too large, do not modify drastically the predictions of the model. Indeed, the data taken in the experiment in [3], which used a $\simeq 180$ fs pulse as a pump for PDC, showed a very good agreement with the model predictions [3]. These conditions ensures that for all the $\vec{w}_0$ in the fast domain, the phase mismatch function can be approximated as

$$\mathcal{D}(\vec{w}, \vec{w}_0 - \vec{w}) l_c \overset{QS}{\to} \mathcal{D}(\vec{w}, -\vec{w}) l_c \quad \forall \vec{w}_0 \in \mathcal{S}_0 \tag{S12}$$

Substituting the QS approximation (S9) in Eq. (S7), we are now in conditions of making some simplifications:

$$\begin{aligned} \langle \hat{B}_1(\vec{w}) \hat{B}_1(\vec{w}_0 - \vec{w}) \rangle &\overset{QS}{\to} \chi_F(\Omega) \chi_F(\Omega_0 - \Omega) h^{\Delta z}(\vec{w}) h^{\Delta z}(\vec{w}_0 - \vec{w}) \mu_{corr}(\vec{w}_0) \Phi_{\rm PDC}(\vec{w}, -\vec{w}) \\ &\simeq \chi_F(\Omega) \chi_F(-\Omega) h^{\Delta z}(\vec{w}) h^{\Delta z}(-\vec{w}) \mu_{corr}(\vec{w}_0) \Phi_{\rm PDC}(\vec{w}, -\vec{w}) \\ &= \chi_F(\Omega) h^{\Delta z}(\vec{w}) h^{\Delta z}(-\vec{w}) \mu_{corr}(\vec{w}_0) \Phi_{\rm PDC}(\vec{w}, -\vec{w}) \end{aligned} \tag{S13}$$

where we assumed that the filtered bandwidth $\Delta\Omega$ is much larger than the width of μ_{corr}, so that $\chi_F(\Omega_0 - \Omega) \approx \chi_F(-\Omega) = \chi_F(\Omega)$ This constraint is not strictly necessary and can be easily relaxed in numerical calculations, but it makes the analytical derivation substantially simpler and cleaner. Moreover, as we have seen, the entangled SHG signal is enhanced by a broadband entanglement of the source, and the scheme is optimized when $\Delta\Omega \simeq 2\Omega_{\rm D} \gg \Omega_{corr}$. Notice that instead the request that the filter is symmetric with respect to ω_1 is crucial to preserve the entanglement, because energy conservation imposes that the frequencies of paired photons are symmetrically displaced.

Let us now turn to the propagator $h^{\Delta z}$. In a separate publication [4] the problem of the propagation of the photonic entanglement away from the source will be discussed at length; here we just sketch the results useful for this work. First, in the QS conditions, terms on the order Ω_0/ω_1 can be safely neglected with respect to 1 (we keep instead terms on the order Ω/ω_1 even though they are small). Then:

$$h^{\Delta z}(\vec{w}_0 - \vec{w}) = \exp\left[i \frac{\Delta z}{2k_{1v}} \frac{q^2 + q_0^2 - 2\vec{q}_0 \cdot \vec{q}}{1 - \frac{\Omega}{\omega_1}} \right] \simeq \exp\left[i \frac{\Delta z}{2k_{1v}} \frac{q^2}{1 - \frac{\Omega}{\omega_1}} \right] \tag{S14}$$

This approximation holds because the distances that optimize the scheme are at most on the order $\frac{1}{2n_1}(l_c + l'_{\rm c}) < 1$ mm in our examples (see the insets of Fig. 5). Then, the term $\sim \frac{q_0^2}{2k_{1v}} \Delta z$, which describes the diffraction of the PDC beam envelope is for sure negligible (for example, a beam of transverse size $D_1 = 300\,\mu$m diffracts on distances on the order of $\frac{\pi D_1^2}{\lambda_1} = 274$ mm). Most important, also the term that couple the fast and slow variables $\sim \frac{q_0 \cdot \vec{q}}{k_{1v}} \Delta z$ can be neglected [4]. By ispection of Eq. (S13), it becomes relevant only when $\Delta z > z_{\rm VCZ}$, where $z_{\rm VCZ} \simeq \frac{l_{\rm D} D_1}{\lambda_1}$ set the boundary of the so-called *deep Fresnel region*, where also the classical coherence properties of the source do not change upon propagation [5, 6]. For the 2 mm BBO described in Fig.2, $l_{\rm D} = 14\,\mu$m, so that for a transverse beam size $D_1 = 300\,\mu$m, $z_{\rm VCZ} = 4.1$ mm. For the 0.5 mm BBO, $l_{\rm D} = 7\,\mu$m and $z_{\rm VCZ} = 2$ mm, but in this case the distances that optimize the scheme are much shorter, on the order $200\,\mu$m. The more detailed analysis in [4] will show that the approximation (S13) can be extended over longer distances, but for our purposes is sufficient to observe that Δz is confined to the deep Fresnel zone from the source.

We use next the fact that the correlation peak μ_{corr} dies out on the fast scale, so that Eq. (S12) holds. Under these conditions, one also has that

$$\mu_{corr}(\vec{w}_0) \Phi_{\rm SHG}(\vec{w}, \vec{w}_0 - \vec{w}) \overset{QS}{\to} \mu_{corr}(\vec{w}_0) \Phi_{\rm SHG}(\vec{w}, -\vec{w}) \tag{S15}$$

as long as the SHG crystal is not longer than the PDC crystal, $l'_{\rm c} \leq l_{\rm c}$, a condition which is anyway necessary to ensure a high efficiency of the upconversion of the PDC radiation. Using this result, and substituting the propagated biphoton amplitude (S13) into Eq. (S6), one gets

$$\langle \hat{a}_2(\vec{w}_0) \rangle \overset{QS}{\to} \mu_{corr}(\vec{w}_0) \int \frac{d^3 w}{(2\pi)^{\frac{3}{2}}} \chi_F(\Omega) h^{\Delta z}(\vec{w}) h^{\Delta z}(-\vec{w}) \Phi_{\rm SHG}(\vec{w}, -\vec{w}) \Phi_{\rm PDC}(\vec{w}, -\vec{w}) \tag{S16}$$

Finally, the mean value of the complete SH field is obtained as

$$\langle \hat{A}_2(\vec{w}_0)\rangle = e^{ik_{2z}(\vec{w}_0)l'_c}\mu_{corr}(\vec{w}_0)\int \frac{d^3w}{(2\pi)^{\frac{3}{2}}}\chi_F(\Omega)h^{\Delta z}(\vec{w})h^{\Delta z}(-\vec{w})\Phi_{\rm SHG}(\vec{w},-\vec{w})\Phi_{\rm PDC}(\vec{w},-\vec{w}) \tag{S17}$$

Under the assumptions of the QS model, μ_{corr} is narrow enough that effects of temporal dispersion and diffraction along $l'_c \leq l_c$ can be neglected, so that $k_{2z}(\vec{w}_0)l'_c \simeq (k_2 + k'_2\Omega_0 - \rho q_{0x})l'_c$. When trasforming back to the real space-time domain, these phase factors simply give rise to time and space shifts, which can be eliminated by setting the origin of the time coordinate at the moment at which the SH wave-packet center exits the medium, and that of the transverse coordinate at the position of the SH pulse center (which is slightly displaced with respect to the position of the fundamental because of walk-off). Thus, in the space-time domain, the mean value of the SH field reads:

$$\begin{aligned}\langle \hat{A}_2(\vec{\xi})\rangle &= e^{ik_2l'_c}\int \frac{d^3w_0}{(2\pi)^{\frac{3}{2}}}\, e^{i\vec{w}_0\cdot\vec{\xi}}\mu_{corr}(\vec{w}_0)\times \\ &\qquad \int \frac{d^3w}{(2\pi)^{\frac{3}{2}}}\chi_F(\Omega)h^{\Delta z}(\vec{w})h^{\Delta z}(-\vec{w})\Phi_{\rm SHG}(\vec{w},-\vec{w})\Phi_{\rm PDC}(\vec{w},-\vec{w}) &\text{(S18)}\\ &= e^{ik_2l'_c}F_{corr}(\vec{\xi})\int \frac{d^3w}{(2\pi)^3}\chi_F(\Omega)h^{\Delta z}(\vec{w})h^{\Delta z}(-\vec{w})\Phi_{\rm SHG}(\vec{w},-\vec{w})\Phi_{\rm PDC}(\vec{w},-\vec{w}) &\text{(S19)}\end{aligned}$$

In this way, we recover equation (24) of the main ms, providing the coherent component of the second harmonic intensity distribution at the NL_2 output:

$$\begin{aligned}\mathcal{I}^{(E)}_{\rm SH}(\vec{\xi}) &= \langle \hat{A}_2^\dagger(\vec{\xi})\rangle\,\langle \hat{A}_2(\vec{\xi})\rangle \\ &= F^2_{corr}(\vec{\xi})\left|\int \frac{d^3w}{(2\pi)^3}\chi_F(\Omega)h^{\Delta z}(\vec{w})h^{\Delta z}(-\vec{w})\Phi_{\rm SHG}(\vec{w},-\vec{w})\Phi_{\rm PDC}(\vec{w},-\vec{w})\right|^2 &\text{(S20)}\end{aligned}$$

B. Incoherent component

We now turn our attention to the incoherent component of the upconverted radiation, with the aim of deriving Eq. (25) of the main manuscript. The incoherent signal originates from the second and third term at r.h.s of Eq. (S4). By inserting them into Eq. (S2) one gets:

$$\begin{aligned}\left\langle \hat{a}_2^\dagger(w'_0)\hat{a}_2(\vec{w}_0)\right\rangle^{inc} &= \int\int \frac{d^3w\,d^3w'}{(2\pi)^3}\big\{\Phi^*_{\rm SHG}(\vec{w}',\vec{w}'_0-\vec{w}')\Phi_{\rm SHG}(\vec{w},\vec{w}_0-\vec{w}) \\ &\qquad \big[\langle \hat{B}_1^\dagger(\vec{w}')\hat{B}_1(\vec{w})\rangle\langle \hat{B}_1^\dagger(\vec{w}'_0-\vec{w}')\hat{B}_1(\vec{w}_0-\vec{w})\rangle \\ &\qquad + \langle \hat{B}_1^\dagger(\vec{w}')\hat{B}_1(\vec{w}_0-\vec{w})\rangle\langle \hat{B}_1^\dagger(\vec{w}'_0-\vec{w}')\hat{B}_1(\vec{w})\rangle\big]\big\} &\text{(S21)}\\ &= 2\int\int \frac{d^3w\,d^3w'}{(2\pi)^3}\big\{\Phi^*_{\rm SHG}(\vec{w}',\vec{w}'_0-\vec{w}')\Phi_{\rm SHG}(\vec{w},\vec{w}_0-\vec{w}) \\ &\qquad \langle \hat{B}_1^\dagger(\vec{w}')\hat{B}_1(\vec{w})\rangle\langle \hat{B}_1^\dagger(\vec{w}'_0-\vec{w}')\hat{B}_1(\vec{w}_0-\vec{w})\rangle\big\} &\text{(S22)}\end{aligned}$$

where we used the fact that the second term under the integral in Eq. (S21) can be obtained from the first one by simply exchanging the coordinates $\vec{w} \leftrightarrow \vec{w}_0 - \vec{w}$. We hence exploit the symmetry of the SHG amplitude with respect to the exchange of its arguments, $\Phi_{\rm SHG}(\vec{w},\vec{w}_0-\vec{w}) = \Phi_{\rm SHG}(\vec{w}_0-\vec{w},\vec{w})$, and, after renaming the integration variables, we obtain Eq. (S22).

The calculation of the integral in Eq. (S22) now relies on the properties of the classical coherence function of the PDC radiation. Under the quasi stationary approximation studied in [1, 2], the coherence function at the output of NL_1 takes the factorized form:

$$\left\langle \hat{C}_1^\dagger(\vec{w}\,')\hat{C}_1(\vec{w})\right\rangle = \mu_{coh}(\vec{w}-\vec{w}\,')\,|V(\vec{w})|^2 \tag{S23}$$

where $|V(\vec{w})|^2$ is the Fourier intensity distribution of the PDC light, defined in Eq. (15), variying on the slow scales $\Omega_{\rm D}$ and $Q_{\rm D}$. In turn

$$\mu_{coh}(\vec{w}) = \int \frac{d^3\xi}{(2\pi)^3}F_{coh}(\xi)e^{-i\vec{w}\cdot\vec{\xi}}, \qquad \text{with } F_{coh}(\vec{\xi}) = \frac{\sinh^2\left[g\mathcal{A}_p(\vec{\xi})\right]}{\sinh^2 g}, \tag{S24}$$

is a well localized coherence peak, which has a fast decay on the scales:

$$\Omega_{coh} = \frac{1}{\tau_p}\sqrt{\frac{4g}{\tanh g}} \ll \Omega_{\rm D}; \qquad\qquad q_{coh} = \frac{1}{w_p}\sqrt{\frac{4g}{\tanh g}} \ll Q_{\rm D} \tag{S25}$$

At high enough gain, the coherence and correlation peaks have the same size (see equation (S11)), while at low gain $g \ll 1$ the coherence is a factor $\sqrt{2}$ larger, but we shall still refer to the narrow region where the coherence function is localized as the *fast* (compared to the scale of variation of $|V|^2$) domain $\mathcal{S}_0$.

For the sake of clarity, let us introduce in in Eq. (S22) the "difference" variables $\Delta\vec{w} = \vec{w} - \vec{w}'$ and $\Delta\vec{w}_0 = \vec{w}_0 - \vec{w}_0'$. By using Eq. (S23) and inserting the propagation between the two crystals, the coherence function entering into the integral in Eq. (S22) becomes:

$$\begin{aligned}\langle \hat{B}_1^\dagger(\vec{w} - \Delta\vec{w})\hat{B}_1(\vec{w})\rangle &\overset{QS}{\to} \chi_F(\Omega - \Delta\Omega)\chi_F(\Omega)\left[h^{\Delta z}(\vec{w} - \Delta\vec{w})\right]^\star h^{\Delta z}(\vec{w})\,\mu_{coh}(\Delta\vec{w})\,|V(\vec{w})|^2 \\ &\simeq \chi_F(\Omega)\mu_{coh}(\Delta\vec{w})\,|V(\vec{w})|^2 \end{aligned} \tag{S26}$$

where, $\mu_{coh}(\Delta\vec{w})$ forces $\Delta\vec{w} = (\Delta\vec{q}, \Delta\Omega)$ to be in the narrow domain (S25). As in the former section, we assume that the filtered bandwidth is much broader than the coherence width Ω_{coh}, so that $\chi_F(\Omega - \Delta\Omega) \simeq \chi_f(\Omega)$. For the propagator, by neglecting terms on the order Ω_{coh}/ω_1, one has:

$$\left[h^{\Delta z}(\vec{w} - \Delta\vec{w})\right]^\star h^{\Delta z}(\vec{w}) = \exp\left(i\frac{\Delta z}{2k_{1v}}\frac{2\vec{q}\cdot\Delta\vec{q} - \delta q^2}{1 + \frac{\Omega}{\omega_1}}\right) \simeq 1 \tag{S27}$$

because, as discussed in the previous section, the optimal distance Δz is short enough that the input of NL_2 is in the deep Fresnel zone of the source, where the light coherence properties remain substantially unchanged upon propagation. Using the same arguments, one also gets:

$$\langle \hat{B}_1^\dagger(\vec{w}_0 - \Delta\vec{w}_0 - \vec{w} + \Delta\vec{w})\hat{B}_1(\vec{w}_0 - \vec{w})\rangle \overset{QS}{\to} \chi_F(\Omega_0 - \Omega)\mu_{coh}(\Delta\vec{w}_0 - \Delta\vec{w})\,|V(\vec{w}_0 - \vec{w})|^2 \tag{S28}$$

The presence of $\mu_{coh}(\Delta\vec{w})$ and $\mu_{coh}(\Delta\vec{w}_0 - \Delta\vec{w})$ under the integral in Eq. (S22) forces $\Delta\vec{w} \simeq 0$ and $\Delta\vec{w}_0 - \Delta\vec{w} \simeq 0$ on the slow scale of phase matching, so that it is possible to approximate:

$$\begin{aligned}&\mu_{coh}(\Delta\vec{w})\mu_{coh}(\Delta\vec{w}_0 - \Delta\vec{w})\Phi^*_{\rm SHG}(\vec{w} - \Delta\vec{w}, \vec{w}_0 - \Delta\vec{w}_0 - \vec{w} + \Delta\vec{w}) \overset{QS}{\to} \\ &\qquad\qquad \mu_{coh}(\Delta\vec{w})\mu_{coh}(\Delta\vec{w}_0 - \Delta\vec{w})\Phi^*_{\rm SHG}(\vec{w}, \vec{w}_0 - \vec{w})\end{aligned} \tag{S29}$$

as long as $l_{\rm c}' < l_{\rm c}$. By inserting these approximations into Eq. (S22), and making the change of variables $\{\vec{w}, \vec{w}'\} \to \{\vec{w}, \Delta\vec{w} = \vec{w} - \vec{w}'\}$:

$$\begin{aligned}\left\langle \hat{a}_2^\dagger(w_0 - \Delta\vec{w}_0)\hat{a}_2(\vec{w}_0)\right\rangle^{inc} &= 2\int d^3\Delta w\; \mu_{coh}(\Delta\vec{w})\mu_{coh}(\Delta\vec{w}_0 - \Delta\vec{w}) \\ &\quad\times \int \frac{d^3w}{(2\pi)^3}\,|\Phi_{\rm SHG}(\vec{w}, \vec{w}_0 - \vec{w})|^2\,|V(\vec{w})V(\vec{w}_0 - \vec{w})|^2 \qquad \text{(S30)} \\ &= 2\int d^3\xi\; F^2_{coh}(\vec{\xi})\, e^{-i\Delta\vec{w}_0\cdot\vec{\xi}} \\ &\quad\times \int \frac{d^3w}{(2\pi)^6}\,|\Phi_{\rm SHG}(\vec{w}, \vec{w}_0 - \vec{w})|^2\,|V(\vec{w})V(\vec{w}_0 - \vec{w})|^2 \qquad \text{(S31)}\end{aligned}$$

where in the second line the definition (S24) of μ_{coh} was used in order to perform the convolution integral over $\Delta\vec{w}$. We are now in conditions of calculating the space-time intensity distribution as:

$$\begin{aligned}\left\langle \hat{A}_2^\dagger(\vec{\xi})\hat{A}_2(\vec{\xi})\right\rangle^{inc} &= \int\int \frac{d^3w_0\, d^3\Delta\vec{w}_0}{(2\pi)^3}\left\langle \hat{a}_2^\dagger(w_0 - \Delta\vec{w}_0)\hat{a}_2(\vec{w}_0)\right\rangle^{inc} e^{i\vec{\xi}\cdot\Delta\vec{w}_0} \\ &= 2F^2_{coh}(\vec{\xi})\int d^3\vec{w}_0 \int \frac{d^3w}{(2\pi)^6}\,|\Phi_{\rm SHG}(\vec{w}, \vec{w}_0 - \vec{w})|^2\,|V(\vec{w})V(\vec{w}_0 - \vec{w})|^2 \\ &= 2F^2_{coh}(\vec{\xi})\int\int \frac{d^3w_1\, d^3w_2}{(2\pi)^6}\,|\Phi_{\rm SHG}(\vec{w}_1, \vec{w}_2)|^2\,|V(\vec{w}_1)V(\vec{w}_2)|^2 \end{aligned} \tag{S32}$$

where, as in the previous section, we properly reset the origin of the space-time coordinate frame at the center of the SH pulse, and neglected terms of order higher then linear in the fast variable $\Delta\vec{w}_0$ in the phase factor $(k_{2z}(\vec{w}_0) - k_{2z}(\vec{w}_0 - \Delta\vec{w}_0))l_{\rm c}'$. In the last line we simply renamed the integration variables to make the result identical to the equation (25) of the main manuscript.

2. EFFICIENCY OF SHG FROM ENTANGLED PHOTONS, PULSED CASE

In order to underline analogies and differences with previous studies, in the main manuscript the efficiency of SHG was mainly studied by considering detection of the peak intensity of the SH signal, which makes sense in the CW case, but clearly is not the best choice in the pulsed case. Moreover, we remind, the quantum advantage is significantly larger when the entire SH pulse, instead of its peak, is detected. In the pulsed case, one is led to consider:

$$N_{\mathrm{SH}} = \sigma_1^{\mathrm{E}} N_{\mathrm{PDC}} + \sigma_2^{\mathrm{E}} N_{\mathrm{PDC}}^2 + \sigma_2^{\mathrm{inc}} N_{\mathrm{PDC}}^2, \tag{S33}$$

where N_{PDC} is the number of PDC photons in a pulse, obtained by integrating the intensity in Eq. (29) over the pulse:

$$N_{\mathrm{PDC}} = \int d^3\xi F_{coh}(\vec{\xi}) \int \frac{d^3w}{(2\pi)^3} |V(\vec{w})|^2 \tag{S34}$$

For our choice of the classical reference, this is also the mean number of photons of the classical pulse at the fundamental frequency. Equation (S33) has to be then compared with the classical upconversion relationship:

$$N_{\mathrm{SH}}^{(cl)} = \sigma_{\mathrm{cl}} N_{\mathrm{PDC}}^2, \qquad \text{with } \sigma_{\mathrm{cl}} = \beta_{\mathrm{cl}} \frac{\int d^3\vec{\xi}\, F_{coh}^2(\vec{\xi})}{\left[\int d^3\vec{\xi}\, F_{coh}(\vec{\xi})\right]^2} \propto \frac{\beta_{\mathrm{cl}}}{\pi D_1^2 T_1} \tag{S35}$$

where we used Eq. (33) for the number of SH photons per pulse in the classical case, and $\pi D_1^2 T_1$ is roughly speaking the spatiotemporal volume of the fundamental pulse at ω_1, which for our choice of the classical reference, coincides with the volume of the quantum pulse.
Taking into account the results for the number of SH photons per pulse in equations (26) and (27), the coefficients of Eq. (S33) can be easily obtained from those in Eq. (36), as

$$\sigma_1^{\mathrm{E}} = \beta_1^{\mathrm{E}} \frac{\int d^3\vec{\xi}\, F_{corr}^2(\vec{\xi})}{\int d^3\vec{\xi}\, F_{coh}(\vec{\xi})} \tag{S36}$$

$$\sigma_2^{\mathrm{E}} = \beta_2^{\mathrm{E}} \frac{\int d^3\vec{\xi}\, F_{corr}^2(\vec{\xi})}{\left[\int d^3\vec{\xi}\, F_{coh}(\vec{\xi})\right]^2} = \frac{\beta_2^{\mathrm{E}}}{\beta_{\mathrm{cl}}} \sigma_{\mathrm{cl}} \frac{\int d^3\vec{\xi}\, F_{corr}^2(\vec{\xi})}{\int d^3\vec{\xi}\, F_{coh}^2(\vec{\xi})} \tag{S37}$$

$$\sigma_2^{\mathrm{inc}} = \beta_2^{\mathrm{inc}} \frac{\int d^3\vec{\xi}\, F_{coh}^2(\vec{\xi})}{\left[\int d^3\vec{\xi}\, F_{coh}(\vec{\xi})\right]^2} = \frac{\beta_2^{\mathrm{inc}}}{\beta_{\mathrm{cl}}} \sigma_{\mathrm{cl}} \tag{S38}$$

Figure S1 illustrates the behaviour of these coefficients at increasing parametric gain, and for

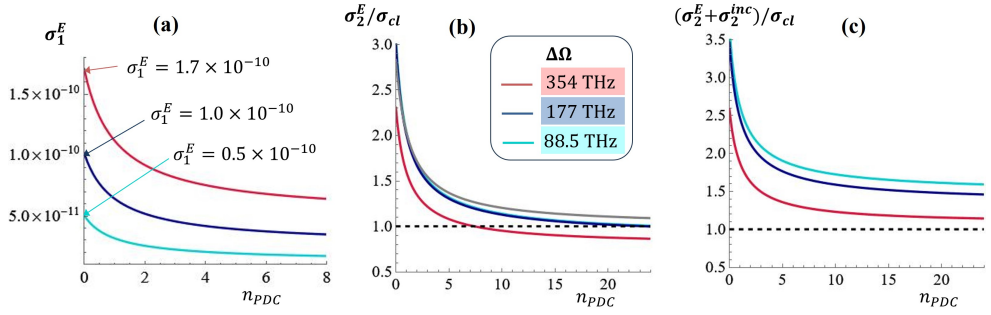

Fig. S1. Efficiency of SHG from entangled photons, from Eq. (S33), for different bandwidths $\Delta\Omega$ of the entangled source, indicated by the legend in (b). (a) Coefficient σ_1^{E} of the linear term. (b) Coefficient σ_2^{E} of the quadratic term, scaled to the classical coefficient σ_{cl}. The gray line is the limit optimal behaviour described by Eq. (S40).(c) Total quadratic efficiency, including coherent and incoherent processes. Parameters as in Fig. 2.

different bandwiths trasmitted on the SHG crystal. For the linear coefficient, a semianalytic approximations of the integrals in Eq. (S36) shows that

$$\sigma_1^{\mathrm{E}} \approx \beta_1^{\mathrm{E}} \left(\frac{1+0.3\,n_{\mathrm{PDC}}}{1+0.7\,n_{\mathrm{PDC}}}\right)^{\frac{3}{2}} \to \begin{cases} \beta_1^{\mathrm{E}} & \text{for } n_{\mathrm{PDC}} \to 0 \\ 0.28\,\beta_1^{\mathrm{E}} & \text{for } n_{\mathrm{PDC}} \to \infty \end{cases} \tag{S39}$$

Hence, σ_1^{E} has the same properties as β_1^{E}: in particular, when the scheme is fully optimized for the coherent upconversion of entangled photons [1], it is proportional to the Fourier volume occupied by entangled modes, or inversely proportional to the entanglement volume in direct space (see the discussion in Sec. 6), but it slowly decreases with gain.
In turn, when the scheme is optimized so that the limit behaviours of Eq. (37) holds, the quadratic coefficient σ_2^{E} has the following behaviour:

$$\begin{aligned}\sigma_2^{\mathrm{E}} &\to \sigma_{\mathrm{cl}} \left[\frac{\int d^3w \left|\overline{\Phi}_{\mathrm{PDC}}(\vec{w},-\vec{w})\right|}{\int d^3w \left|\overline{V}(\vec{w})\right|^2} \right]^2 \frac{\int d^3\vec{\xi}\, F_{corr}^2(\vec{\xi})}{\int d^3\vec{\xi}\, F_{coh}^2(\vec{\xi})} \\ &\approx \sigma_{\mathrm{cl}} \left(2\,\frac{1+0.32\,n_{\mathrm{PDC}}}{1+0.64\,n_{\mathrm{PDC}}} \right)^{\frac{3}{2}} \to \begin{cases} 2\sqrt{2}\,\sigma_{\mathrm{cl}} & \text{for } n_{\mathrm{PDC}} \to 0 \\ \sigma_{\mathrm{cl}} & \text{for } n_{\mathrm{PDC}} \to \infty \end{cases}\end{aligned} \tag{S40}$$

where the function of n_{PDC} in the second line comes from a seminalytic fit of the spatiotemporal integrals in Eq. (S37). The behaviour described by Eq. (S40) is shown by the gray curve in Fig. S1. As for β_2^{E}, for the two smaller bandwidths σ_2^{E} stays close enough to this optimal limit, while, when the bandwith is too large with respect to $2\Omega_{\mathrm{D}}$ (red curve, $\Delta\Omega = 354\,\mathrm{THz}$), it undergoes a significant reduction because of dispersion broadening of biphotons. Notice that the quadratic efficiency shown in Fig. S1 is much larger than that in Fig. 6b, corresponding to detection of the peak intensity, because, as already remarked, the peak value of the entangled SH signal underestimates the number of entangled pairs upconverted. This in turn corresponds to a true enhancement of the quadratic SHG rate due to entanglement, because the coefficient has been normalized to its classical counterpart σ_{cl}.
Finally, panel (c) of Fig. S1 shows the total quadratic SHG efficiency, including both coherernt and incoherent processes. From Eq. (S38), we have that $\sigma_2^{\mathrm{inc}}/\sigma_{\mathrm{cl}} = \beta_2^{\mathrm{inc}}/\beta_{\mathrm{cl}} \simeq$ costant with gain, hence the curve in panel c are simply the curves in panel b shifted up by a costant value. As a result, in all these examples (even for the red curve, in which the bandwidth is not optimal) the quadratic rate of SHG from PDC photons is always larger than its classical counterpart

REFERENCES

1. A. Gatti, O. Jedrkiewicz, and E. Brambilla, "Modeling the space-time correlation of pulsed twin beams," Sci. Rep. **13**, 16786 (2023).
2. A. Gatti, E. Brambilla, and O. Jedrkiewicz, "Unified space-time description of pulsed twin beams," Philos. Transactions Royal Soc. A: Math. Phys. Eng. Sci. **382**, 20230334 (2024).
3. T. Dickinson and et al., "Quantum-enhanced two-photon processes beyond the photon pairs regime,"arXiv:2504.15249 [quant-ph] (2025).
4. A. Gatti and E. Brambilla, "Propagation of photonic entanglement in air and tissues," (preprint). Alessandra.gatti@ifn.cnr.it.
5. R. Cerbino, "Correlations of light in the deep Fresnel region: An extended Van Cittert and Zernike theorem," Phys. Rev. A **75**, 053815 (2007).
6. A. Gatti, D. Magatti, and F. Ferri, "Three-dimensional coherence of light speckles: Theory," Phys. Rev. A **78**, 063806 (2008).

[1] i.e., when the two crystals are perfectly tuned, $l_c' < l_c$, the position of NL_2 is set as the optimal one and the bandwith is properly chosen